

# Estimation of Adhesion Hysteresis at Polymer/Oxide Interfaces Using Rolling Contact Mechanics

Hongquan She,<sup>†</sup> David Malotky,<sup>‡</sup> and Manoj K. Chaudhury<sup>\*,†,‡</sup>

Department of Chemical Engineering and Polymer Interface Center, Lehigh University, Bethlehem, Pennsylvania 18015

Received September 22, 1997. In Final Form: February 9, 1998

The rolling of a cylinder on a flat plate can be viewed as the propagation of two cracks—one closing at the advancing edge and the other opening at the trailing edge. The difference of adhesion in these two regions, i.e. the adhesion hysteresis, depends on the nonequilibrium interfacial processes in an elastic system. This rolling contact geometry was used to study the effects of dispersion forces and specific interactions on interfacial adhesion hysteresis. In order to accomplish this objective, hemicylindrical elastomers of polydimethylsiloxane (PDMS)—both unmodified and plasma oxidized—were rolled on thin PDMS films bonded to silicon wafers. Plasma oxidation generates a silica-like surface on PDMS elastomer, which interacts with PDMS molecules via hydrogen-bonding forces. The adhesion hysteresis in the latter case is large and depends significantly on the molecular weight of the grafted polymer, whereas the hysteresis is rather negligible for purely dispersive systems. These results are interpreted in terms of the orientation and relaxation of polymer chains, which has its origin in the Lake–Thomas effect.

## Introduction

When a deformable curved object is brought into contact with another curved or flat substrate, the adhesion forces tend to deform the solids and thus increase their area of contact. At equilibrium, the area of contact is determined by the balance of elastic, potential, and surface energies of the whole system. For a sphere in contact with a flat plate, the work of adhesion ( $W$ ) can be expressed as follows:<sup>1</sup>

$$W = (Ka^3/R - P)^2 / (6\pi Ka^3) \quad (1)$$

where  $a$  is the radius of the contact circle,  $R$  is the radius of curvature of the sphere,  $P$  is the external load, and  $K$  is defined as

$$1/K = (3/4)\{(1 - \nu_1^2)/E_1 + (1 - \nu_2^2)/E_2\} \quad (2)$$

$\nu_i$  and  $E_i$  are the Poisson ratios and elastic moduli of the two objects. A mechanical calibration of the load-deformation ( $P$  vs  $a$ ) data allows simultaneous determination of  $W$  and  $K$  from eq 1. The corresponding equation for a cylinder with its axis lying parallel to a flat plate is<sup>2,3</sup>

$$W = [(3\pi Kb^2/8R) - P]^2 / (6\pi Kb^2) \quad (3)$$

where  $2l$  is the length of cylinder and  $2b$  is the width of the contact deformation. The contact mechanics of spherical geometries has been used extensively to study adhesion between various deformable elastic materials.<sup>4–29</sup>

By contrast, the cylinder–flat plate geometry is a relatively new system to study adhesion between deformable objects. The advantage of this geometry is that the cylinder can be rolled<sup>30–33</sup> on the flat surface, thus simulating a peeling situation that is free from many complexities associated with the mechanics of peeling a tape or a ribbon. The rolling cylinder geometry also has the advantage that the experiment can be performed at constant rates of crack propagation, which is complementary to the experiments involving the sphere–sphere or sphere–flat plate contacts.

(7) Lee, A. E. *J. Colloid Interface Sci.* **1978**, *64*, 577.

(8) Horn, R. G.; Israelachvili, J. N.; Pribac, F. *J. Colloid Interface Sci.* **1987**, *115*, 480.

(9) Chaudhury, M. K.; Whitesides, G. M. *Langmuir* **1991**, *7*, 1013.

(10) Chaudhury, M. K.; Owen, M. J. *J. Phys. Chem.* **1993**, *97*, 5722.

(11) Chaudhury, M. K.; Whitesides, G. M. *Science* **1992**, *255*, 1230.

(12) Chaudhury, M. K. *J. Adhesion Sci. Technol.* **1993**, *7*, 669.

(13) Haidara, H.; Chaudhury, M. K.; Owen, M. J. *J. Phys. Chem.* **1995**, *99*, 8681.

(14) Mangipudi, V.; Tirrell, M.; Pocius, A. V. *J. Adhesion Sci. Technol.* **1994**, *8*, 1251.

(15) Merrill, W. W.; Pocius, A. V.; Thakkar, B.; Tirrell, M. *Langmuir* **1991**, *7*, 1975.

(16) Deruelle, M.; Leger, L.; Tirrell, M. *Macromolecules* **1995**, *28*, 1995.

(17) Kendall, K. *J. Adhesion* **1973**, *5*, 179.

(18) Chen, Y. L.; Helm, C. A.; Israelachvili, J. N. *J. Phys. Chem.* **1991**, *95*, 10737.

(19) Silberzan, P.; Perutz, S.; Kramer, E. J.; Chaudhury, M. K. *Langmuir* **1994**, *10*, 2466.

(20) Shanahan, M. E. R.; Michel, J. *Int. J. Adhesion* **1991**, *11*, 170.

(21) Vallat, M. F.; Ziegler, P.; Vondracek, P.; Schultz, J. *J. Adhesion* **1991**, *35*, 95.

(22) Rimai, D. S.; DeMejo, L. P.; Bowen, R. C. *J. Appl. Phys.* **1990**, *68*, 6234.

(23) Bowen, R. C.; Rimai, D. S.; DeMejo, L. P. *J. Adhesion Sci. Technol.* **1989**, *3*, 623.

(24) DeMejo, L. P.; Rimai, D. S.; Bowen, R. C. *J. Adhesion Sci. Technol.* **1988**, *2*, 331; **1991**, *5*, 959.

(25) Creton, C.; Brown, H. R.; Shull, K. R. *Macromolecules* **1994**, *27*, 3174.

(26) Perutz, S.; Kramer, E. J.; Baney, J.; Hui, C. Y. *Macromolecules* **1997**, *30*, 7964.

(27) Brown, H. R. *IBM J. Res. Dev.* **1994**, *38*, 379.

(28) Ahn, D.; Shull, K. R. *Macromolecules* **1996**, *29*, 4381.

(29) Maugis, D.; Barquins, M. *J. Phys. Lett.* **1981**, *L95*, 42.

(30) Roberts, A. D.; *Rubber Chem. Tech.*, **1979**, *52*, 23.

(31) Kendall, K. *Wear* **1975**, *33*, 351.

(32) Charmet, J.; Verjus, C.; Barquins, M. *J. Adhesion* **1996**, *57*, 5.

(33) Barquins, M. *J. Natl. Rubber Res.* **1990**, *5*, 199.

\* To whom correspondence should be addressed.

<sup>†</sup> Polymer Interface Center.

<sup>‡</sup> Department of Chemical Engineering.

(1) Johnson, K. L.; Kendall, K.; Roberts, A. D. *Proc. R. Soc. London, A* **1971**, *324*, 301.

(2) Barquins, M. *J. Adhesion* **1988**, *26*, 1.

(3) Chaudhury, M. K.; Weaver, T.; Hui, C. Y.; Kramer, E. J. *J. Appl. Phys.* **1996**, *80* (1), 30.

(4) Kendall, K. *J. Phys. D: Appl. Phys.* **1973**, *5*, 1782; **1973**, *8*, 1449; *Proc. R. Soc. London, A*, **1975**, *341*, 409; **1975**, *344*, 287; *J. Adhesion* **1975**, *7*, 137; *J. Mater. Sci.* **1976**, *11*, 638; **1975**, *10*, 1011.

(5) Roberts, A. D.; Othman, A. B. *Wear* **1977**, *42*, 119.

(6) Tabor, D. *J. Colloid Interface Sci.* **1977**, *58*, 2.

In the past,<sup>30–33</sup> it has been shown that the rolling cylinder geometry is convenient in studying the adhesive and frictional properties of deformable elastic materials. Here, we have used this method to study an important problem in surface chemistry, namely, to examine what roles do the dispersion and nondispersion (e.g. H-bonding) forces play in adhesion and how that is influenced by the molecular weight of the polymer. The theoretical approach used here to analyze the rolling contact data is adapted from the earlier works of Johnson<sup>34</sup> and particularly, that of Barquins,<sup>33</sup> as discussed below.

**Rolling Contact and Adhesion Hysteresis.** When a compliant hemispherical cylinder is brought into contact with another rigid substrate, a rectangular deformation occurs spontaneously in the contact zone. The width of the rectangle is a measure of the balance of the elastic, potential, and surface energies of the whole system. In this case, the distribution of the normal stress in the contact area is symmetric about the center line of contact. The stress is maximally compressive at the center but has singular tensile values at the edges of contact, which are supported by the adhesion forces of the two surfaces. What happens when such a cylinder rolls on the flat plate? Two possible scenarios can emerge. The case of rolling can be viewed as the propagation of two cracks, one closing at the advancing edge and the other opening at the trailing (receding) edge. If the energy necessary to close the crack is exactly the same as that needed to open the crack, the distribution of the normal stress in the contact zone remains unaffected by the rolling action and the contact width ( $2b$ ) does not change. In the case of two surfaces interacting with each other via London dispersion forces, as is the case with a cross-linked silicone rubber cylinder rolling over a low-energy surface, no adhesion hysteresis prevails and the distribution of the normal stress remains symmetric about the center line of contact. The situation changes completely if the silicone elastomer rolls over a hydrogen-bonding surface. The energy needed to open a crack is now significantly higher than that needed to close the crack; consequently, the width of the rolling contact ( $2b$ ) increases from its static value ( $2b_0$ ).

It is shown in this paper that the work of adhesion ( $W_r$ ) in the trailing (receding) edge of a rolling cylinder is related to the work of adhesion ( $W_a$ ) in the advancing edge as follows:

$$W_r = W_a \{2(b/b_0)^{3/2} - 1\}^2 \quad (4)$$

The term in the curly brackets depends upon the irreversible processes occurring at the interface. Derivation of eq 4 starts by recognizing that the distribution of normal stress within the contact zone ( $-\beta, \alpha$ ) in a hysteretic situation is asymmetric<sup>34</sup> (eq 5a):

$$\sigma(x) = \frac{1}{\pi^2 \{(x + \beta)(\alpha - x)\}^{1/2}} \times \int_{-\beta}^{\alpha} \frac{\{(s + \beta)(\alpha - s)\}^{1/2} \left( \frac{\pi E^* s}{2R} \right)}{x - s} ds - \frac{P}{\pi \{(x + \beta)(\alpha - x)\}^{1/2}} \quad (5a)$$

Where,  $\alpha$ ,  $\beta$ , and  $x$  are indicated in Figure 1 and  $s \in (-\beta, \alpha)$ . On the basis of the following coordinate transformation ( $\beta + \alpha = 2b$ ,  $\alpha - \beta = 2d$ ,  $x = r + d$ ) eq 5a becomes<sup>32</sup>

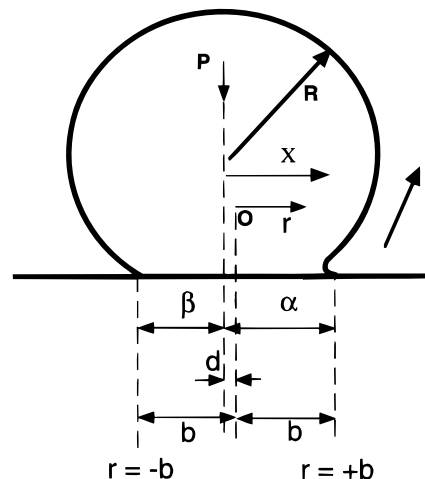


**Figure 1.** Schematic of a cylinder rolling on a flat plate counterclockwise. Here, the cylinder is deformable and the flat plate is rigid. Adapted from ref 32.

$$\sigma(r) = \frac{-\frac{P}{\pi} + \left( \frac{E^*}{2R} \right) \left( r^2 + rd - \frac{b^2}{2} \right)}{(b^2 - r^2)^{1/2}} \quad (5b)$$

where,  $1/E^* = (1 - \nu_1^2)/E_1 + (1 - \nu_2^2)/E_2$ .  $P$  is the external load acting on the cylinder per unit length.  $R$  is the principal radius of curvature of the cylinder, and  $d$  is indicated in Figure 1.  $r$  is the distance within the contact zone measured from the center line of contact. Here we use the convention that  $r = -b$  and  $r = +b$  correspond to the location of advancing and receding edges, respectively. It can be shown that the normal stresses at  $r = \pm b$  have square root singularities. For example, as  $r$  approaches  $+b$ ,  $\sigma(r)$  becomes

$$\sigma(r \rightarrow +b) = (1/2b)^{1/2} \{-P/\pi + (E^*/2R)(b^2/2 + bd)\}/(b - r)^{1/2} \quad (6)$$

The mode I stress intensity factor ( $K_I$ ) is

$$K_I = \lim_{r \rightarrow +b} \sigma(r) [2\pi(b - r)]^{1/2} = (\pi/b)^{1/2} [-P/\pi + (E^*/2R)(b^2/2 + bd)] \quad (7)$$

The parameter  $d$  can be related to the torque ( $\tau$ ) needed to roll the cylinder by the following integral:

$$-\tau = \int_{-b}^{+b} \sigma(r)(r + d) dr \quad (8a)$$

or

$$d = \tau / [\pi E^* b^2 / (4R) - P] \quad (8b)$$

In plane strain, the mode I strain energy release rate ( $G$ ) is

$$G = K_I^2 / 2E^* \quad (9)$$

Identifying  $G$  with the receding work of adhesion  $W_r$  in the trailing (receding) edge, eqs 7, 8b, and 9 can be combined to yield

$$P + (2\pi E^* b W_r)^{1/2} = (\pi E^* b^2 / 4R) + 2\tau/b + 8\tau PR / (\pi E^* b^3) \quad (10)$$

A similar approach at  $r \rightarrow -b$  yields

(34) Johnson, K. L. *Contact Mechanics*; Cambridge University Press: Cambridge, 1985.

$$P + (2\pi E^* b W_a)^{1/2} = (\pi E^* b^2/4R) - 2\tau/b - 8\tau PR/(\pi E^* b^3) \quad (11)$$

where  $W_a$  is the advancing work of adhesion.

Elimination of  $\tau$  from eqs 10 and 11 yields eq 12.

$$W_a^{1/2} + W_r^{1/2} = 2\{(\pi E^* b^2/4R) - P\}/(2\pi E^* b)^{1/2} \quad (12)$$

Equation 12 is the desired equation to analyze the rolling contact data, but it can be further simplified. When the cylinder is first brought into contact with the flat sheet at zero load, i.e. before rolling, the contact equilibrium<sup>2,3</sup> can be described as follows:

$$W_a^{1/2} = (\pi E^* b_0^2/4R)/(2\pi E^* b_0)^{1/2} \quad (13)$$

where  $b_0$  is the half-width of the rectangular contact area in the static case, which increases to  $b$  when rolling occurs. In a typical rolling experiment, without any additional external load, the value of  $P$  is found to be only about 1–4% of  $\pi E^* b^2/4R$ , and thus it can be safely neglected. Using this simplification, eqs 12 and 13 can be combined to yield eq 4. The values of  $W_a$  and  $W_r$  can be separately and rigorously determined from eqs 10 and 11 if the rolling torque ( $\tau$ ) is measured in conjunction with  $P$  and  $b$ . Alternatively, eq 4 can be used to estimate the value of  $W_r$ , provided that the value of  $W_a$  is known. In this paper we have used the latter procedure.

The basic question, which we investigated in this study, is how the van der Waals and nondispersive interactions contribute to adhesion hysteresis in polymeric systems. The subject has its origin in the Lake–Thomas<sup>35</sup> effect. In the fracture of cross-linked (and entangled) polymers, it is observed that the fracture energy increases with the molecular weight. Lake and Thomas argued that all the chemical bonds between the cross-linking points are excited to higher energy states. When one bond breaks, all the other bonds return to their ground states, thus releasing energy proportional to the number of bonds between cross-linking or entanglement points. The basic predictions of Lake and Thomas have been verified in a number of earlier studies by Gent and Tobias<sup>36</sup> as well as by Carre and Schultz.<sup>37</sup> More recently, Creton et al.<sup>25</sup> have used the Lake–Thomas<sup>35</sup> argument (improved further by Raphael and de Gennes<sup>46</sup>) to address the effects of grafting density and molecular weight of polymers in chain pull-out from an elastic network. Shanahan and Michel<sup>20</sup> as well as Vallat et al.<sup>21</sup> have used the JKR method to study the adhesion between cross-linked rubbers and glass and found that the adhesion energy increases with the inter-cross-link molecular weight ( $M_c$ ) of the rubbers. According to these authors, the rubber molecules are oriented in the immediate vicinity of the crack tip. The entropic free energy due to chain orientation is dissipated following relaxation of these chains during crack extension. As a first approximation, one may envisage that this energy dissipation is proportional to the inter-cross-link molecular weight of the rubber. In this paper, we have re-examined some of the findings of the above authors by studying the adhesion between silica and polydimethylsiloxane (PDMS) using the method of rolling contact mechanics.

**Model Systems Used To the Study Lake–Thomas Effect.** Thin PDMS films were formed by reacting

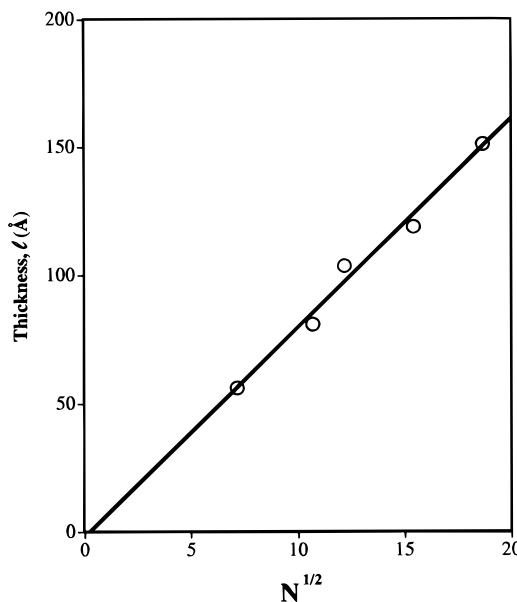


**Figure 2.** Thickness ( $l$ ) of the PDMS film grafted onto silicon versus the square root of the number of monomers ( $N$ ) per chain. The regression analysis yields  $l = 8.2N^{1/2} \pm 2.0 \text{ \AA}$ .

hydrosilane functional PDMS polymers  $(\text{HSi}(\text{CH}_3)_2(\text{OSi}(\text{CH}_3)_2)_n(\text{CH}_2)_3\text{CH}_3)$  with a self-assembled monolayer of undecenylsilane supported onto silicon wafers using a platinum catalyst. The thicknesses of these PDMS films are proportional to the square root of the molecular weights of the polymer (Figure 2). These surface-modified silicon wafers will henceforth be referred to as Si-PDMS. The PDMS hemicylinders were used in both unoxidized and oxidized forms. Oxidation of PDMS was carried out in an oxygen plasma at a reduced pressure, which generated a thin ( $<50 \text{ \AA}$ ) silica-like layer on the surface of the polymer.<sup>38</sup> Low-angle XPS showed that the chemical composition of the surface of oxidized PDMS elastomer is that of silica ( $\text{SiO}_x$ ). The oxidized PDMS cylinders will henceforth be referred to as PDMS<sup>ox</sup>. The atmospheric water adsorbs and reacts with silica to form silanol groups, which interact with the siloxane groups of the grafted PDMS chains via specific (nondispersive) molecular forces. Although no direct experiment has been done to elucidate the nature of this specific interaction, there are good reasons to believe that PDMS interacts with silica by very weak H-bonding forces.<sup>3,38</sup> The rolling data were analyzed using eq 4, with the value of  $W_a$  fixed at  $44 \text{ mJ/m}^2$ . The above value of  $W_a$  was estimated using the conventional JKR method by measuring the deformations produced on contacting hemispherical lenses of PDMS<sup>ox</sup> to Si-PDMS. The hemispherical lens of PDMS was brought into contact with the Si-PDMS surface at zero load, and then the load was continuously increased to  $100 \text{ dyn}$  at a loading rate of about  $0.1 \text{ dyn/s}$ . At the end of this loading experiment, the lens was unloaded at the same rate until it pulled out of Si-PDMS. These load-deformation data were analyzed using the JKR equation in the following format:

$$a^{3/2}/R = (P/Ka^{3/2}) + (6\pi W/K)^{1/2} \quad (14)$$

According to eq 14, a plot of  $a^{3/2}/R$  versus  $P/a^{3/2}$  should yield a straight line, the slope and intercept of which depend on the magnitudes of  $K$  and  $W$ . Figure 3 summarizes the results obtained with two representative

(35) Lake, G. J.; Thomas, A. G. *Proc. R. Soc. London, A* **1967**, *300*, 108.

(36) Gent, A. N.; Tobias, R. H. *J. Polym. Sci., Polym. Phys. Ed.* **1982**, *20*, 2051.

(37) Carre, A.; Schultz, J. *J. Adhesion* **1984**, *17*, 135.

(38) Fakes, D. W.; Davies, M. C.; Browns, A.; Newton, J. M. *Surf. Interface Anal.* **1988**, *13*, 233.

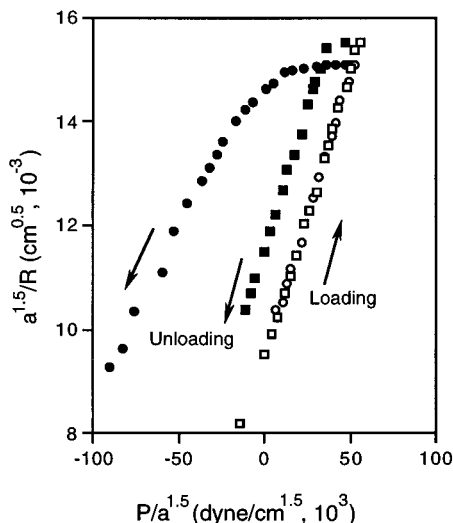


**Figure 3.** Load-deformation data of oxidized hemispherical PDMS<sup>ox</sup> lenses on grafted films of PDMS of two molecular weights plotted according to eq 14. □ (loading) and ■ (unloading) correspond to the PDMS film of MW 3882; ○ (loading) and ● (unloading) correspond to the molecular weight 11 080. Note that, for both the polymers, the loading data fall on the same straight line, whereas the unloading data exhibit adhesion hysteresis. Hysteresis increases with the molecular weight.

Si-PDMS surfaces. The loading branches for two different molecular weights of PDMS fall on the same straight line, indicating identical values of  $W_a$ . Experiments performed with a number of unoxidized and oxidized PDMS lenses show that the values of  $W_a$  always cluster around 44 mJ/m<sup>2</sup>, which was used as the representative value for  $W_a$  (eq 4) in the analysis of the rolling contact data. From the complete cycles of load-deformation behavior, it is apparent that all the nonequilibrium interfacial processes become manifest only during the unloading branch. The loading branch, on the other hand, is governed by the reversible thermodynamic work of adhesion, which is almost the same as twice the surface free energy of PDMS (22 mJ/m<sup>2</sup>). The unloading (or receding) works of adhesion at PDMS<sup>ox</sup> and Si-PDMS interfaces were examined in detail as a function of the contact time and molecular weight of the grafted polymer using the rolling contact mechanics, as described below.

## Results and Discussion

**Rolling Contact.** When a hemicylinder of PDMS<sup>ox</sup> was brought into contact with Si-PDMS, a rectangular deformation ( $-b_0, +b_0$ ) occurred in the zone of contact, which was measured with a microscope using reflection optics (Figure 4). When this cylinder was tilted on one of its edges, the width of the rectangle increased to a certain value before the cylinder started to roll. During rolling, the receding edge propagated from  $+b_0$  to  $-b_0$ , whereas the advancing edge propagated beyond  $-b_0$  (Figure 5).

As the cylinder started to roll, the tilted flat end of the cylinder caused the rays of light emanating from the contact zone to refract, causing the positions of both the parallel boundaries of the rectangle to shift slightly. This shift of optical image gave the false impression that the trailing edge receded before it actually did. In various control tests, we found that this unavoidable optical artifact was not detrimental to the accurate measurement of the width ( $2b$ ) of the rectangle. A number of variables affected the rolling results. The most significant variables were the time of contact and the ambient humidity. In order to minimize the effect of humidity, the whole

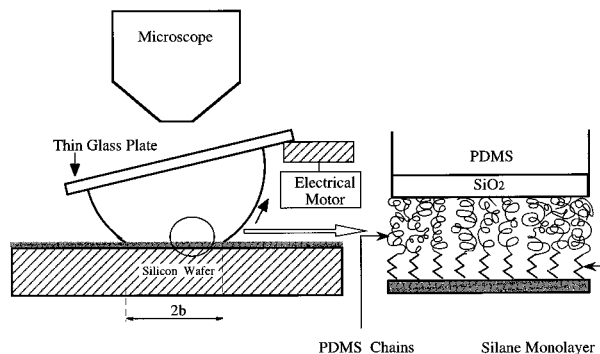


**Figure 4.** Schematic of the rolling contact apparatus. An oxidized PDMS hemicylinder is brought into contact with PDMS chains grafted onto silicon. The adhesion energy is dictated by the adsorption of the PDMS chains onto the silica-like layer of oxidized PDMS. When the hemicylinder is tilted on one of its edges, it starts to roll. The width at rolling is a measure of adhesion hysteresis.

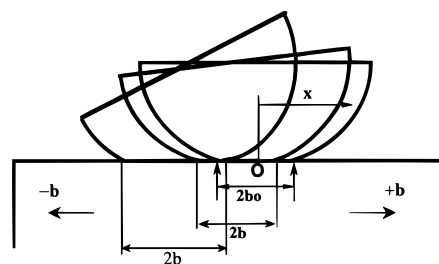


**Figure 5.** Exaggerated view of the rolling of a hemicylinder on a flat plate.

instrument was encased inside a Plexiglass box that was constantly purged with predried air, which ensured the humidity inside the box would remain fixed at 20%. The PDMS hemicylinders were oxidized using oxygen plasma in order to generate thin silica (SiO<sub>2</sub>) films on their surfaces. After oxidation, the cylinders were equilibrated with the internal humidity (20%) of the Plexiglass box for 40 min. These hemicylinders were then placed upon the test substrates (Si-PDMS) for different amounts of time before the rolling experiments were conducted (Figure 4). The  $W_r$  values were obtained from the rolling contact data using eq 4. In order to check the validity of the  $W_r$  values obtained from the rolling experiments, a separate control experiment was performed as follows. In that, the plasma-oxidized PDMS hemicylinders were contacted with the test substrate (Si-PDMS) under a compressive load of 0.02 N for fixed amounts of time and then the load was reduced to zero. From the equilibrium values of the contact widths,  $W_r$  values were calculated using eq 3, the validity of which had already been established in a previous publication.<sup>2</sup> The above unloading and rolling experiments yielded comparable values of  $W_r$ . For example, the  $W_r$  values obtained from the unloading and rolling experiments with PDMS<sup>ox</sup> in contact with a PDMS film ( $M = 11\ 080$ ) were 125 and 120 mJ/m<sup>2</sup>, respectively, for a contact time of 2 min.

These values increased to 290 mJ/m<sup>2</sup> (unloading) and 300 mJ/m<sup>2</sup> (rolling) for a contact time of 10 min. These agreements of the  $W_r$  values obtained from two different methods provide reasons to believe that eq 4 is correct. Furthermore, eq 4 shows that the estimation of  $W_r$  does not depend on the radius of curvature of the cylinder. PDMS<sup>ox</sup> cylinders of various radii of curvature (0.15–0.80 cm) were rolled over a PDMS film ( $M = 11\ 080$ ) after an initial contact time of 10 min. The corresponding works of adhesion ( $W_r$ ) clustered around 310 ( $\pm 15$ ) mJ/m<sup>2</sup>,

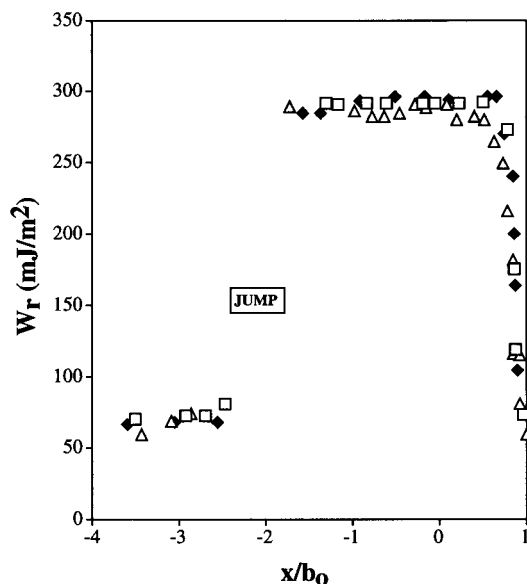


**Figure 6.** Receding work of adhesion ( $W_r$ ) obtained from the rolling of PDMS<sup>ox</sup> on PDMS film (MW = 11 080) at different crack velocities. (□) 28  $\mu\text{m/s}$ ; ( $\Delta$ ) 43  $\mu\text{m/s}$ ; ( $\blacklozenge$ ) 62  $\mu\text{m/s}$ . The PDMS<sup>ox</sup> cylinder was rolled after it contacted the film for 10 min. Note that  $W_r$  does not depend on the crack velocity. The jump is illustrated in Figure 7.

indicating that there is no significant effect of the radius of curvature on the estimation of  $W_r$ . Figure 6 shows the results of rolling a PDMS<sup>ox</sup> cylinder over a Si-PDMS surface. When the trailing edge travels from  $+b_0$  to  $-b_0$ , the work of adhesion increases to a plateau value, which increases with the time of contact. This contact-time-dependent adhesion gives rise to a spectacular instability in rolling as discussed below.

**Instability in Rolling Contact.** As the cylinder of PDMS<sup>ox</sup> rolls over Si-PDMS, new interfacial contact is made at the advancing edge whereas the contact is broken at the receding edge. The time allowed to make new contact is, however, significantly smaller than the resident time of contact before rolling. Hence, there is a discontinuity of the adhesion energy ( $W_r$ ) at the juncture of old and new contacts (at  $b = -b_0$ ), which is experienced by the trailing edge when it travels from  $+b_0$  to  $-b_0$ . This discontinuity of  $W_r$  causes an elastic instability, and thus the cylinder rolls abruptly to a new position ( $x < -b_0$ ) with a corresponding decrease in the contact width (Figure 7). Figure 6 shows how the work of adhesion  $W_r$  varies as the trailing edge recedes. The rates of crack propagation, in these experiments, were 28–62  $\mu\text{m/s}$ . In this range,  $W_r$  is rather insensitive to the crack propagation rate. Note that, after the elastic instability, the receding work of adhesion decreases to about 50–60  $\text{mJ/m}^2$ , a value close to that of  $W_a$  (44  $\text{mJ/m}^2$ ), thus indicating that the work of adhesion between PDMS<sup>ox</sup> and Si-PDMS is governed mainly by dispersion forces at short contact time.

As the contact time increases, the siloxane of Si-PDMS starts interacting with PDMS<sup>ox</sup> with nondispersive (most likely, H-bonding) forces; consequently,  $W_r$  increases. Figure 8 shows plots of the normalized work of adhesion as a function of contact time for three different molecular weights of PDMS. The work of adhesion initially increases at a fast rate for up to 30 min of contact, after which  $W_r$  changes very slowly. The above interfacial reconstruction may be viewed as mediated by an adsorption process<sup>39,40</sup>

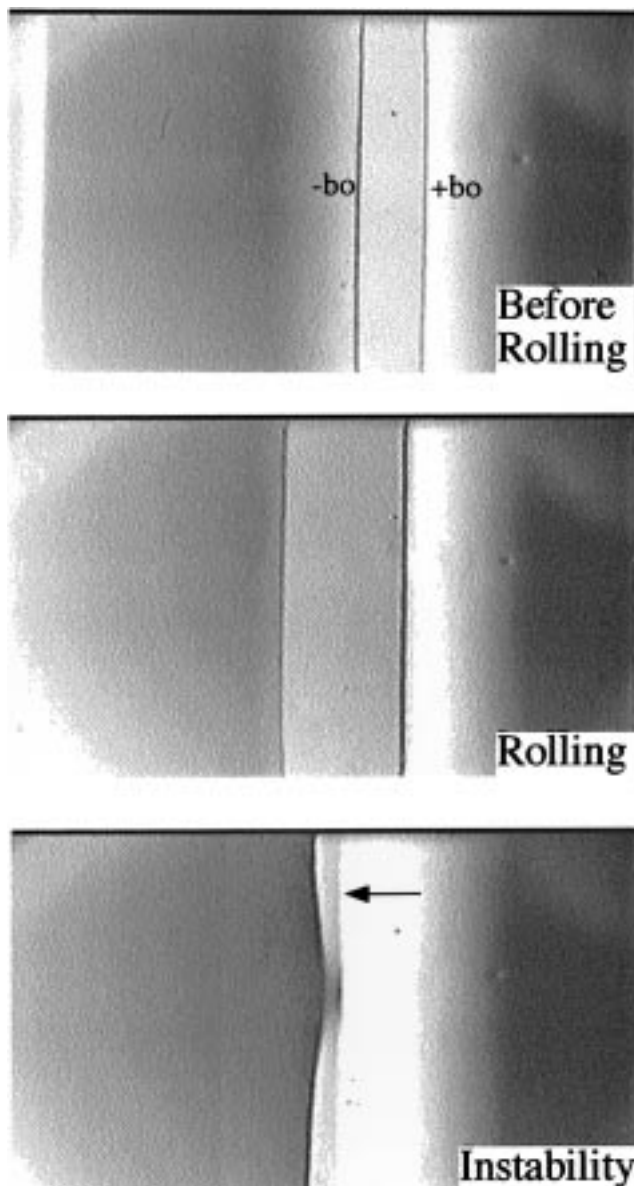


**Figure 7.** Video prints of the different phases of contact of a PDMS<sup>ox</sup> cylinder on Si-PDMS (MW = 11 080). As the receding edge reaches the discontinuity of the old and new contact (see arrow), an instability occurs in rolling and the cylinder jumps to a new position. The advancing edge is not seen clearly in the figure after the onset of instability. Note that the instability appears to take place at  $-1.5b_0$  instead of  $-b_0$ . This shift of optical image is due to the refraction of light from the hemicylindrical lenses, as discussed in the text.

leading to a progressive saturation of the surface sites of PDMS<sup>ox</sup>. The near independence of the process on molecular weight indicates that it is controlled by local segmental level adsorption–desorption processes at the polymer/silica interface.

#### Effect of Molecular Weight of Grafted Polymer.

The plateau values (200–2000  $\text{mJ/m}^2$ ) of the work of adhesion increase almost linearly up to the molecular weight 17 670 but rise to a much higher value at the molecular weight 25 840 (Figure 9). What is the origin of such high values of  $W_r$  considering the fact that the advancing work of adhesion for these cases is only about 44  $\text{mJ/m}^2$ ? On the basis of some approximate values of the nondispersive enthalpy of adsorption ( $\approx 1 \text{ kT}$ ) of

(39) Cohen-Addad, J. P.; Huchot, P.; Jost, P.; Pouchelon, A. *Polymer* **1989**, *30*, 143.

(40) Girard, O.; Cohen-Addad, J. P. *Polymer* **1991**, *32* (5), 860.

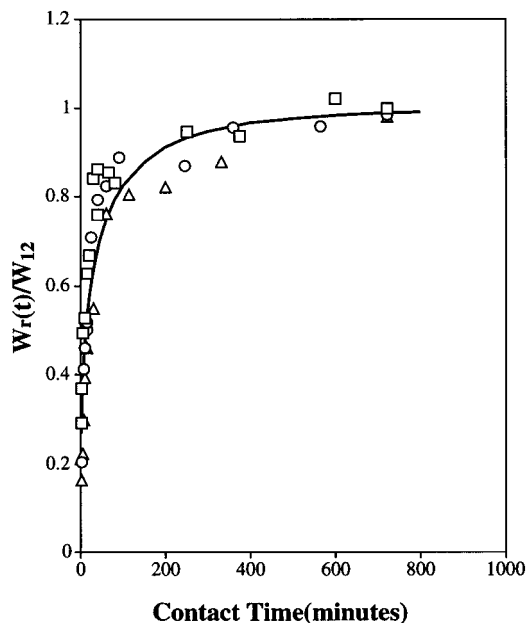


**Figure 8.** Normalized receding work of adhesion versus contact time for three different molecular weights of PDMS. The values of the work of adhesion were divided by the work of adhesion obtained after 12 h of contact ( $W_{r12}$ ). The values of  $W_{r12}$  are 209, 607, and 1950  $\text{mJ/m}^2$ , respectively, for molecular weights of 3882 ( $\square$ ), 11 080 ( $\circ$ ), and 25 840 ( $\triangle$ ).

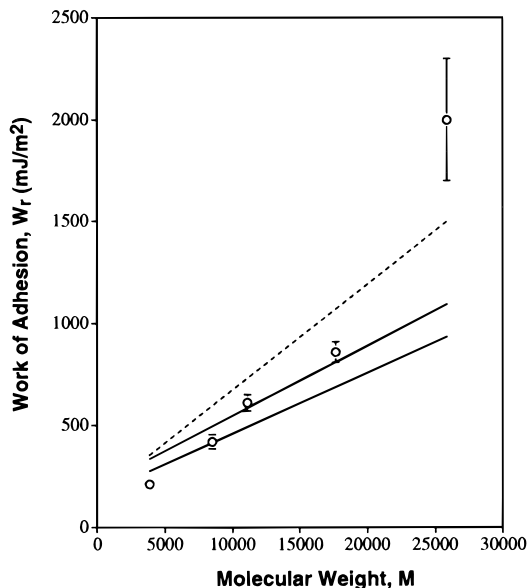


**Figure 9.** Receding work of adhesion ( $W_r$ ) of PDMS<sup>ox</sup> on PDMS films of different molecular weights. Open circles ( $\circ$ ) indicate the experimental adhesion data obtained after 12 h of contact for a crack velocity of 28  $\mu\text{m/s}$ . Solid lines are the adhesion energies calculated from eq 22 with the value of  $f_c$  as 25 pN (lower line) and 50 pN (upper line). The dashed line indicates the adhesion energies calculated using the persistence chain model with the value of  $f_c$  as 25 pN.

siloxane on silica<sup>39</sup> and the number of free silanol groups<sup>41</sup> per unit area ( $1.8 \times 10^{-2} \text{ \AA}^{-2}$ ), we estimate that the nondispersive work of adhesion between PDMS and silica is about 7.2  $\text{mJ/m}^2$ , which is significantly smaller than the dispersion force component of the work of adhesion (44  $\text{mJ/m}^2$ ). In order to provide another perspective to the problem, let us examine how PDMS interacts with another hydrogen-bonding material—water. The inter-

(41) Zhuravlev, L. T. *Langmuir* **1987**, *3*, 316.

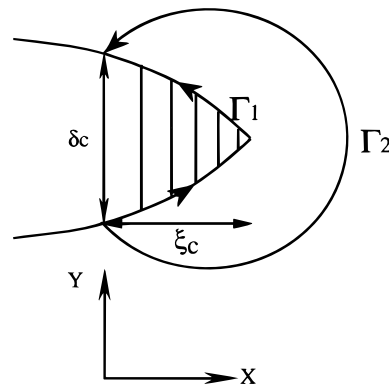


**Figure 10.** Cohesive zone of a crack. Here,  $\xi_c$  is the section of the cohesive zone which is bridged by polymer chains.

facial tension<sup>42</sup> between PDMS and water is about 44  $\text{mJ/m}^2$ . Using this value of the interfacial tension, the work of adhesion between PDMS and water is estimated to be about 50  $\text{mJ/m}^2$ , of which 44  $\text{mJ/m}^2$  comes from dispersion interaction, thus leaving only 6  $\text{mJ/m}^2$  for the nondispersive interaction. This analysis suggests, as well, that the nondispersive interaction between PDMS and water is very weak. In order to estimate the nondispersive component of the interaction between PDMS and silica, we have used microflow calorimetry.<sup>43</sup> The experiments were performed by flowing a solution of PDMS in isooctane over silica powders and measuring the heat of adsorption. The dispersive component of the enthalpy of adsorption of PDMS on  $\text{SiO}_2$  should be screened in isooctane; thus, whatever heat of adsorption is measured should primarily be due to nondispersive interactions. For PDMS of five different molecular weights ( $M = 3882, 8520, 11080, 17670, 25840$ ), the values of heat of adsorption clustered around 120–150  $\text{mcal}$  per gram of silica. From these adsorption enthalpies and surface area of silica, the enthalpy of adhesion between PDMS and silica is estimated to be about 13–16  $\text{mJ/m}^2$ . It should be mentioned here that even though the enthalpy of interaction of PDMS with silica is very small, the polymer chains could not still be desorbed from silica when the fluid phase was changed back to pure isooctane. Clearly, the high fracture energies obtained for PDMS/silica systems cannot be explained on the basis of adsorption energies alone.

We believe that the explanation for the high value of  $W_r$  at the PDMS/ $\text{SiO}_2$  interface lies in the Lake–Thomas<sup>35</sup> effect. The basic idea of Lake and Thomas can be understood using the concept of Barenblatt's<sup>44</sup> cohesive zone and Rice's  $J$ -integral<sup>45</sup> method of evaluating the energy release rate. Rice introduced an intergral ( $J$ ) defined as

$$J = \int_{\Gamma} \left( \epsilon \, dy - \mathbf{T} \frac{\partial \mathbf{u}}{\partial x} \, ds \right) \quad (15)$$

where  $\epsilon$  is the strain energy density,  $\Gamma$  is a curve surrounding the crack tip,  $\mathbf{T}$  is the traction vector,  $\mathbf{u}$  is the displacement vector, and  $ds$  is an element of arc length along  $\Gamma$ .  $\Gamma$  can be any path surrounding the crack from its lower surface to the upper surface in a counterclockwise direction (Figure 10). Rice demonstrated that the value

(42) Kanellopoulos, A. G.; Owen, M. J. *Trans. Faraday Soc.* **1971**, *67*, 3127.

(43) Fowkes, F. M.; Dwight, D. W.; Cole, D. A.; Huang, T. C. *J. Non-Cryst. Solids* **1990**, *120*, 47.

(44) Barenblatt, G. I. *Adv. Appl. Mech.* **1962**, *7*, 55.

(45) Rice, J. R. *J. Appl. Mech. Trans. ASME* **1968**, *90*, 379.

(46) Raphael, E.; de Gennes, P. G. *J. Phys. Chem.* **1992**, *96*, 4002–4007.

of  $J$  is path independent; i.e.,  $J_{\Gamma_1} = J_{\Gamma_2}$ . Evaluation of  $J$  along path  $\Gamma_2$  yields the elastic strain energy release rate ( $G$ ). However, when path  $\Gamma_1$  is chosen,  $J$  becomes<sup>45</sup> the interfacial energy release rate:

$$J = - \int_{\Gamma_1} \mathbf{T} \frac{\partial \mathbf{u}}{\partial \mathbf{x}} \cdot \mathbf{ds} = \int_0^{\delta_c} \sigma(\delta) \, d\delta \quad (16)$$

where  $\sigma(\delta)$  is the restraining stress between the open surfaces of the crack. When the van der Waals interactions provide the only restraining force, the above value of  $J$  becomes the conventional Dupre work of adhesion. However, if the two crack faces are restrained by polymer bridges, Rice argued that  $\sigma(\delta)$  is contributed by the elastic tensions in the chains.

As the molecular weight of the bridging polymer increases, it increases the values of  $\delta_c$  and thus  $J$ , as has been observed in our experiments. Next, we provide a tentative explanation for the molecular-weight-dependent adhesion shown in Figure 9. When the two crack faces are held by polymer bridges, the interfacial release rate can also be written as follows:

$$W_r = J_{\text{interface}} = \int_0^{\delta_c} \sigma(\delta) \, d\delta = \sum \int_0^{F_c} F \, d\delta(F) \quad (17)$$

where  $\Sigma$  is the number of polymer chains per unit area and  $F(\delta)$  is the force acting on a single polymer chain for a corresponding chain extension of  $\delta$ .  $F_c$  is the critical force at which the chain breaks at its weakest linkage. The force of interaction between a single PDMS chain and  $\text{SiO}_2$  is much weaker than the force needed to break a Si–O–Si bond; hence, the weakest linkage is probably at the PDMS– $\text{SiO}_2$  interface. Note that eq 17 describes the work done in separating the two parallel surfaces from its minimum distance to a point of separation.

It is possible to estimate  $W_r$  with the help of eq 17 provided that the areal density of the load-bearing chains ( $\Sigma$ ), the number of monomers per connector, and the critical force ( $F_c$ ) at which the chain desorbs are known. Since the above variables are not accurately known in our system, we make several simplified assumptions, which allow us to estimate the values of  $W_r$  in a very approximate way. First, we need to consider a simplified model of how the polymer chains stretch and relax in the cohesive zone. Previous studies of Cohen-Addad et al.<sup>40</sup> clearly demonstrated that PDMS, as is the case with macromolecules, adsorbs onto  $\text{SiO}_2$  by multiple segments. In an idealized case, one may picture that the adsorbed chain is detached from  $\text{SiO}_2$  like a zipper. Since the hydrogen bonds are broken sequentially, the detachment process should exhibit a saw-tooth force–distance profile. The energy needed to desorb a single chain can be written approximately as

$$g \approx f_c L_c \quad (18)$$

where  $f_c$  is the force needed to break a single H-bond and  $L_c$  is the contour length of the polymer chain. The total fracture energy then becomes

$$W_r \approx \sum f_c L_c \quad (19)$$

where  $\Sigma$  is taken as the mass-averaged grafting density,  $\rho N_A l / M$ , where  $\rho$  ( $\approx 1 \text{ g/cm}^3$ ) is the density of PDMS,  $N_A$  is Avogadro's number, and  $l$  and  $M$  are the thickness and the molecular weight of the grafted PDMS (Figure 2). Since  $\Sigma \propto M^{-1/2}$  and  $L_c \propto M$ ,  $W_r$  should be proportional to the square root of the molecular weight. However the

experimental data show that  $W_r$  scales at least linearly with  $M$  for  $3882 < M < 17\,670$ .

The above scenario of chain pull-out is however oversimplified. In reality, multiple polymer chains overlap onto a given adsorption area. Thus, when a single polymer chain is pulled, the applied force should be distributed to multiple H-bonds. When a polymer chain having  $N$  monomers adsorbs onto a solid surface from the melt, the adsorbed area is overlapped by  $\sqrt{N}$  other chains.<sup>40</sup> Thus, a single polymer chain, as a first approximation, should be restrained by  $\sqrt{N}$  bonding sites contributed by the segments of the overlapping chains. A similar situation might prevail in the present case; i.e.,  $\sqrt{N}$  H-bonds are activated on the PDMS<sup>ox</sup> surface when a single PDMS chain is pulled.

There are, probably, two levels of amplification of fracture energy—one is due to the molecular weight of polymer (classical Lake–Thomas effect), and the other is due to the multiple H-bonding sites. The overall fracture energy can now be approximated as

$$W_r \approx \sum N(\sqrt{N}\epsilon) \quad (20)$$

where  $\epsilon$  is the average elastic energy released per bond in the separation process. Note that eq 20 predicts that  $W_r$  varies linearly with molecular weight as has been observed experimentally for  $3882 < M < 17\,670$ . The experimental fracture energies (Figure 9) can be explained by eq 20 with a value of  $\epsilon$  on the order of  $kT$ . Clearly, entropic energy is sufficient to explain the adhesion data. Now we provide estimates of the fracture energies on the basis of the entropic theories of chain elasticity. First, we consider the freely jointed chain model, according to which the chain extension  $\delta$  can be expressed as follows<sup>47</sup>

$$\begin{aligned} \delta(F) &= L_c \left[ \coth\left(\frac{aF}{kT}\right) - \frac{kT}{aF} \right] \\ &= L_c \mathcal{L} \left( \frac{aF}{kT} \right) \end{aligned} \quad (21)$$

where  $a$  is the length of each independent segment of the chain and  $k$  and  $T$  are the Boltzmann constant and the absolute temperature, respectively. Using the methods described by Flory,<sup>48</sup>  $a$  is estimated to be  $6.75 \text{ \AA}$  for PDMS, and its contour length is  $3N \text{ \AA}$ , where  $N$  is the degree of polymerization.

Since each chain is anchored to the surface by  $\sqrt{N}$  H-bonds, the threshold force, at which a chain desorbs from  $\text{SiO}_2$ , is on the order of  $N^{1/2} f_c$  (Figure 11). Therefore,  $W_r$  may be estimated from the following equation:

$$W_r = \sum \int_0^{N^{1/2} f_c} F \, d\delta(F) \quad (22)$$

In order to estimate  $W_r$  from eqs 22, we also need to estimate  $f_c$ . We have attempted to measure<sup>49</sup> the force needed to desorb a single PDMS chain from  $\text{SiO}_2$  by using an atomic force microscope (AFM). The details of these measurements will be published elsewhere; here only a brief description is given. In that, an AFM tip, made of  $\text{SiO}_2$ , was brought incrementally toward a PDMS-grafted silicon wafer while carrying out multiple force–distance

(47) Bueche, F. *Physical Properties of Polymers*; Interscience Publishers: New York, 1962.

(48) Flory, P. J. *Statistical Mechanics of Chain Molecules*; Oxford University Press and Hanser Publishers: 1988.

(49) Details of these studies will be published separately.

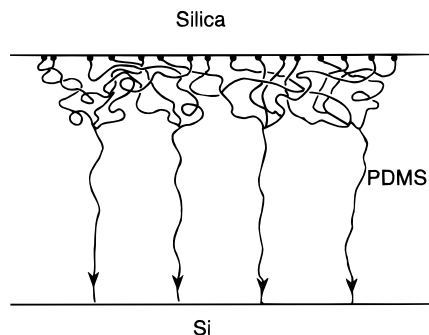


**Figure 11.** Schematic illustration of how the force applied to a single chain might be transmitted to multiple bonding sites on a SiO<sub>2</sub> surface. Polymer chains are thought to overlap each other during the adsorption process which leads to interfacial entanglement. When the polymer chain is pulled, it first slips out of the network. Ultimately both the chain and the network stretch and the force applied to a single chain is distributed to multiple sites.

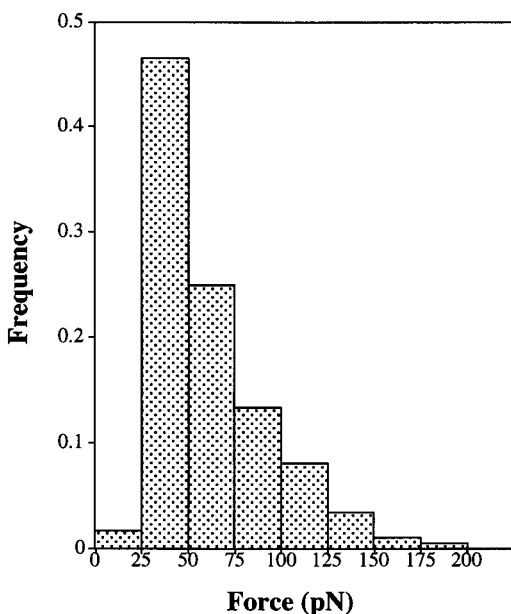


**Figure 12.** Histogram of bonding forces between SiO<sub>2</sub> and Si-PDMS obtained from the AFM measurements. These results were obtained with PDMS of molecular weights 25 840, 17 670, and 11 080.

scans. During these incremental advances, the tip occasionally measures the bonding force with one PDMS chain, which extends above the average thickness of the grafted polymer layer. This method, which was used earlier by Rief et al.<sup>50</sup> to measure interactions in biological systems, worked rather well with PDMS of higher molecular weights (25 840, 17 670, and 11 080) but poorly with PDMS of lower molecular weights. In the later case, it was rather difficult to avoid the AFM tip to snap into the primary energy minimum. The combined distribution of bond forces between the SiO<sub>2</sub> tip and all the high-molecular-weight PDMS films ranges from 25 to 200 pN (Figure 12), with the value 25–50 pN observed most frequently. The values of  $W_f$  were determined using eq 22, where  $f_c$  was taken to be the lowest force (25–50 pN) obtained in the AFM measurements.

As seen in Figure 9, estimated  $W_f$  values scale linearly with  $M$ . The numerical values of  $W_f$  are also close to its experimentally found values. However the estimated  $W_f$

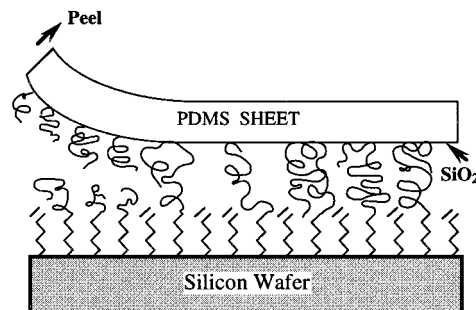


**Figure 13.** Schematic of a peel experiment. An oxidized PDMS sheet is placed on a Si-PDMS surface for a fixed amount of time (12 h), and then it is gently peeled away. The change of thickness of PDMS before and after the peeling provides estimates of chain scission at the surface (not drawn to scale).

~  $M$  line has a slope lower than that observed experimentally. Recently, several direct measurements of chain extension as a function of force on single polymer chains show that the FJC model is inadequate to describe the  $F$ - $\delta$  profile at high extensions.<sup>51</sup> The high-extension data fit rather well with the persistence chain model, according to which  $\delta$  is expressed as follows:<sup>52,53</sup>

$$F = \frac{kT}{A} \left[ 0.25 \left( 1 - \frac{\delta}{L_c} \right) - 0.25 + \frac{\delta}{L_c} \right] \quad (23)$$

where  $A$  is the persistence length of the chain, which is about half of the Kuhn length ( $a$ ). Although the persistence chain model (PCM)<sup>53</sup> was derived mainly to describe the elastic behavior of stiff chains, its use has also been extended to other polymers of very low persistence lengths.<sup>52</sup> The persistence chain model, in our case, overpredicts the values of  $W_f$  somewhat, but the predicted slope of the  $W_f \sim M$  line is in fair agreement with the experimental data. While the applicability of the persistence chain model to flexible PDMS is in serious doubt, it is clear that an appropriate model of chain elasticity that allows extension to approach the contour length more smoothly than the FJC model does would predict the adhesion data reasonably well.

The situation is somewhat unclear for PDMS of  $M = 25\,840$ . Interestingly, the molecular weight of this polymer is close to the critical molecular weight of entanglement (25 000–30 000) of PDMS in the melt. Clearly, other mechanisms for the amplification of fracture energy need to be considered including the possibility of the distortion and scission of the siloxane bonds. There is significant experimental difficulty associated with the assessment of chain scission in the small area of contact used in these contact mechanics experiments. In order to obtain a rough idea of the possibility of chain scission, we have performed a peel experiment, even though the interpretation of the peel data is complicated by the fact that a substantial amount of shear stress develops in the test. In these experiments, flat sheets of plasma-oxidized PDMS were placed on PDMS-grafted silicon wafers (Si-PDMS) for a period of 12 h, after which the sheets were gently peeled away by hand (Figure 13). In these preliminary experiments, even though the peeling speeds were not controlled, they were at least an order of magnitude higher than those used in the rolling contact tests. The change of thickness of the PDMS films was

(51) Smith, S. B.; Finzi, L.; Bustamante, C. *Science* **1992**, *258*, 1122.

(52) Reif, M.; Gautel, M.; Oesterhelt, F.; Fernandez, J. M.; Gaub, H. E. *Science* **1997**, *276*, 1109.

(53) Marko, J. F.; Siggia, E. D. *Macromolecules* **1995**, *28*, 8759–8770.

(50) Rief, M.; Oesterhelt, F.; Heymann, B.; Gaub, H. E. *Science* **1997**, *275*, 1295.

**Table 1. Thickness of PDMS Films before and after the Peeling of a Flat Sheet of PDMS<sup>ox</sup> from Grafted PDMS Films of Different Molecular Weights**

molecular weight	thickness before fracture (Å)	thickness after fracture (Å)
3882	51	46
8520	78	64
11080	102	76
17670	120	89
25840	150	136

measured by ellipsometry. For the lowest molecular weight polymer ( $M = 3882$ ), chain scission is negligible; significant scission occurs for PDMS of MW > 8500 (Table 1). Although a peel test may not be a true representative of the rolling contact test (because of the differences in geometries and test speeds), the evidence of PDMS chain scission, nevertheless, adds another dimension that needs to be accounted for in more refined analysis of these fracture data.

The results of the adhesion experiments in this study and those of the previous adsorption measurements<sup>39,40</sup> suggest that PDMS interacts with such H-bond-forming surfaces as silica and water with some nonspecific forces in addition to the dispersive interactions. What is the nature of this specific interaction? Ulman et al.<sup>54</sup> have recently studied the adhesion of PDMS elastomeric caps with self-assembled monolayers containing such terminal groups as phosphoric acid, carboxylic acid, and alcohol. The authors found that the strength of interaction between PDMS and these SAMs increases with their acidities, suggesting that the oxygen of siloxane forms a hydrogen bond with the protons of the acid groups. One might expect that the methyl groups of the siloxane sterically hinder the oxygen of Si–O–Si from forming such a bond. Nevertheless, since Si–O–Si is a very flexible bond<sup>55</sup> (linearization barrier, 0.3 kcal/mol), it can assume various bond angles (120–180°) without paying significant energetic penalty in the backbone distortion. According to Ross et al.,<sup>56</sup> the silicon atom of PDMS is a weak electron acceptor and the specific interactions that we find with PDMS are due to the acidity of the silicon atom. We feel that a hydrogen bond between siloxane and silica is responsible for the hysteresis that we observe in these systems. We came to this conclusion on the basis of our earlier study, which showed that the hysteresis in the adhesion between PDMS and mica is negligible.<sup>3</sup> Mica does not have any proton-donating group, and hence it cannot form a hydrogen bond with PDMS, whereas the proton-donating silanol of silica can form a significant hydrogen bond with PDMS.<sup>57</sup> The fact that some kind of specific interactions is responsible for the high-adhesion hysteresis at the PDMS–silica interface gains further support from the fact that the hysteresis disappears completely when the surface of PDMS<sup>ox</sup> is further modified with a hydrophobic, low-energy, silane monolayer (CH<sub>3</sub>–(CH<sub>2</sub>)<sub>15</sub>–SiCl<sub>3</sub>). We will refer to this surface as PDMS<sup>ox</sup>–(CH<sub>2</sub>)<sub>15</sub>–CH<sub>3</sub>. As evident in Figure 14, the  $W_r$  values obtained from the rolling of PDMS<sup>ox</sup>–(CH<sub>2</sub>)<sub>15</sub>–CH<sub>3</sub> on Si-PDMS are very close to the values of  $W_a$  (44 mJ/m<sup>2</sup>). These differences between the  $W_r$  values obtained at PDMS<sup>ox</sup>/PDMS and PDMS<sup>ox</sup>–(CH<sub>2</sub>)<sub>15</sub>–CH<sub>3</sub>/PDMS interfaces indicate that the high adhesion value in the former case is due to H-bonding or some other type of specific interactions.

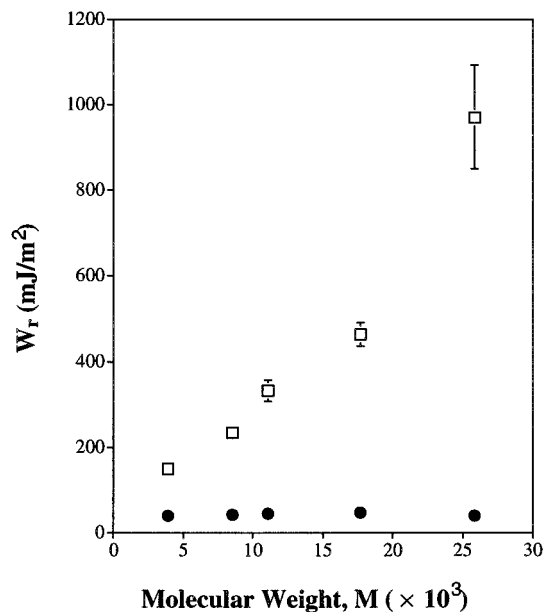


**Figure 14.** Receding work of adhesion ( $W_r$ ) of PDMS<sup>ox</sup> (□) and PDMS<sup>ox</sup>–(CH<sub>2</sub>)<sub>15</sub>–CH<sub>3</sub> (●) on PDMS films of different molecular weights obtained after a contact time of 10 min. Note that the molecular weight influences the fracture energy for H-bonding not for dispersion interaction.

We now conjecture on the differences between the adhesion hysteresis seen with the dispersive and non-dispersive interactions. The difference may be qualitatively understood on the basis of the differences in the energy barriers that exist in the desorption of the polymer chains from the surfaces. Consider Figure 10, where we are interested to find out the section ( $\xi_c$ ) of the cohesive zone that is bridged by the polymer chains. It is this length that determines  $\delta_c$  and thus  $W_r$  (eq 17). The time taken for a polymer chain to stretch from its undeformed length to  $\delta_c$  is the same as the time ( $\xi_c/V$ ) taken for the crack to traverse the length of a cohesive zone. In the absence of any energy barrier, the characteristic time of desorption of a polymer chain is  $h/kT$ , where  $h$  is the Planck's constant.  $\xi_c$  is approximately equal to  $hV/kT$ . Dispersive systems provide little energy barrier to desorption, in which case  $\xi_c$  is vanishingly small at any reasonable crack propagation rate, which is the same as saying that the polymer chains are hardly stretched in the cohesive zone and thus  $\delta_c$  is vanishingly small. The only restraining force operating in the cohesive zone is then the dispersion force, where no adhesion hysteresis prevails. However if the desorption process involves a transition state, the corresponding length of the cohesive zone becomes  $\sim hV/kT e^{\Delta G_a/RT}$ , where  $\Delta G_a$  is the activation free energy of polymer desorption. Assuming arbitrarily a value of  $\Delta G_a$  of 15 kcal/mol, the above length of the cohesive zone becomes 1  $\mu\text{m}$  at a crack velocity of 100  $\mu\text{m/s}$ . Such a large value of  $\xi_c$  means that the value of  $\delta_c$  is also high; thus, a significant amount of restraining stress can be provided in the cohesive zone by the polymer bridges. The fracture energy in this case is higher than that contributed by only the dispersion forces. The energy barrier to the desorption of a single siloxane group from silica is probably not very high. However, the desorption of the adsorbed polymer can be dramatically slowed down because of the adsorption by multiple segments and/or of the steric pinning imposed by other overlapping chains that leads to interfacial entanglement. A kind of slowing down of polymer desorption by steric

(54) Ulman, A. personal communication, 1997.

(55) Durig, J. R.; Flanagan, M. J.; Kalasinsky, V. F. *J. Chem. Phys.* **1977**, *66*, 2775.

(56) Ross, S.; Nguyen, N. *Langmuir* **1988**, *4* (5), 1188.

(57) Chaudhury, M. K. *Mater. Sci. Eng. Rev.* **1996**, *R16*, 97.

pinning was observed earlier by Granick et al.,<sup>58</sup> who showed that the kinetics of desorption, in such a case, follows the Vogel–Fulcher law instead of the simple Eyring's rate law. If indeed the dynamics of PDMS chains slows down in the cohesive zone,  $\xi_c$  becomes long and the corresponding fracture energy increases because of high  $\delta_c$ . The limited set of data shown in Figure 6 indicates that the adhesive fracture energy does not depend significantly on crack speed. These results would make sense if the cohesive zone is completely saturated by the stretched polymer chains at these speeds. This point is illustrated as follows. As mentioned earlier, the length ( $\xi_c$ ) of the cohesive zone is approximately a product of the crack velocity ( $V$ ) and the characteristic relaxation time ( $\tau_r$ ) of polymer desorption (i.e.  $\xi_c = V\tau_r$ ). The fracture energy is however determined by  $\delta_c$  not  $\xi_c$ . The relevant length ( $\xi_c^*$ ) of the cohesive zone is, therefore, such that it can support the connecting chains in the boundary region in their maximally extended configuration ( $\delta_c$ ), the value of which is limited by  $F_c$ . For very slowly relaxing polymer  $\xi_c^* \ll \xi_c$ , in which case the cohesive zone is saturated by stretched polymer chains and the fracture energy does not depend on crack velocity. A more careful analysis of all these issues would have to be made by considering more detailed processes that involve not only the desorption of PDMS from SiO<sub>2</sub> but also polymer chain scission. An evidence of a very slow relaxation kinetics of PDMS in the cohesive zone was obtained in the following experiment. In that, a PDMS<sup>ox</sup> hemicylinder was tilted on a Si-PDMS substrate using a micromanipulator to a sufficient amount that the trailing edge started to recede. At this point, the micromanipulator motion was stopped and the relaxation of the receding contact line was monitored over a period of 1–4 days. It was found that the contact line relaxed slowly over a period of 10 hours, beyond which no noticeable relaxation of the contact line was observed (Figure 15). During this time, the adhesive fracture energy ( $W_f$ ) decreases by only about 50–60%, clearly pointing out that the dynamics of the polymer chain in the cohesive zone is very sluggish.

### Final Remarks

Rolling contact mechanics, as pioneered by Barquins, provides a convenient method to study adhesion between deformable solids. The method was valuable in studying the effects of molecular weight and H-bonding interaction on the adhesion of siloxane polymers to silica surfaces. Our results indicate that a weak interfacial interaction can be amplified dramatically by the molecular weight of the polymer as well as by the multiple attachment sites on SiO<sub>2</sub>, which is consistent with the experimentally observed  $W_f \sim M$  scaling for  $M < 17\,000$ . It is not yet clear what is the origin of the large deviation of  $W_f$  at  $M = 26\,000$ . In terms of the molecular processes occurring in the cohesive zone, there are, clearly, other possibilities to consider. Restraining of a polymer chain by multiple attachment sites has been considered here. In a more refined treatment, it would be necessary to consider the effects of the distortion of siloxane bonds as well as the effect of polymer chain scission.

### Experimental Section

**General Information.** Both the hemicylinders and hemispheres of poly(dimethylsiloxanes) were prepared using a commercial silicone elastomer kit (Dow Corning, Syl-184). The polymers used to modify the surfaces of silicon wafers were hydridofunctional polydimethylsiloxane (HSi(CH<sub>3</sub>)<sub>2</sub>(OSi(CH<sub>3</sub>)<sub>2</sub>)<sub>*n*</sub>

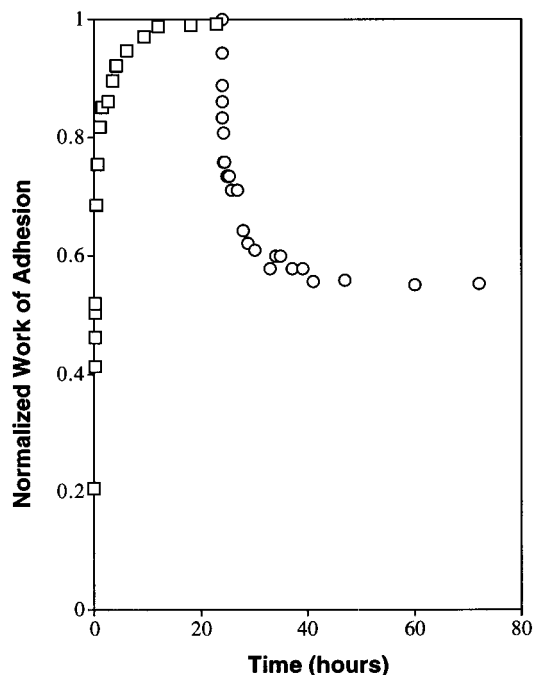


**Figure 15.** How the adhesion between a PDMS ( $M = 11\,080$ ) film and a PDMS<sup>ox</sup> cylinder increases with time and then how the interface relaxes after a rolling torque is applied. The first 24 h of the data is indicative of polymer adsorption, whereas the data obtained after 24 h indicate how polymer desorbs from SiO<sub>2</sub>. Note that the adhesion energy decreases by only about 50% even after 48 h, indicating that the desorption is a very slow process.

(CH<sub>2</sub>)<sub>3</sub>CH<sub>3</sub>) of molecular weights 3882, 8520, 11080, 17670, and 25840 (Dow Corning Corp.), with the respective polydispersity indexes of 1.1, 1.2, 1.2, 1.3, and 1.2. The Whatman Purge Gas Generator (Model 75-62) was obtained from Balston Inc. The microscope used for the rolling contact mechanics and the JKR measurements was purchased from Nikon (Nikon Optiphot) and was equipped with a video camera (MTI-65, DAGE-MTI Inc.), a video monitor (DAGE-MTI, Model HR1000), a micromanipulator (Nikon, Model MM188), and a VCR (SONY, Model SVO-1500). An external motor (Ladd Research Industries, Inc.) was used to fine-control the vertical movement of the micromanipulator. A Mettler (Mettler AC100) analytical balance was used to measure external loads. Plasma oxidation was carried out with a Harrick Plasma Cleaner (Model PDC-32G, 100 W). Contact angles were measured with a modified Ramé Hart goniometer (Model-100). The silicon wafers were purchased from Silicon Quest International. The chloroform (assay > 99.8%) used to clean and extract PDMS was obtained from Fisher Scientific.

**Preparation of PDMS Hemicylinders and Grafted Polymer Layers.** The detailed methods for preparing the PDMS hemicylinders and hemispheres have previously been described in refs 3 and 9. Here only a brief description is given. A 10:1 (w:w) mixture of Syl-184 and curing agent was stirred in a plastic weighing dish. After about 1 h of deaeration, 200  $\mu$ L of the mixture was applied onto the surfaces of fluorocarbon-treated glass cover strips (3 mm  $\times$  60 mm) using a microsyringe. The liquid polymer was contained within the strip and set to elastomer in the shape of a hemicylinder. The curing reaction was carried out first at room temperature for overnight; then the reaction mixture was heated in an oven at 75  $^{\circ}$ C for 2 h. The curved cylinders were removed from the glass strips and extracted with chloroform in a soxhlet extractor for 2 h. After the cylinders were allowed to dry in a vacuum dessicator for a few days, smaller cylinders ( $\approx$ 2 mm) were cut out from the longer cylinder using a sharp razor blade. Hemispheres were made by placing small drops of the same mixture on the fluorinated microscope glass slides. The cured hemispherical lenses had radii of curvature of  $\approx$ 1 mm. The flat sheets of the silicone elastomers were prepared from the same material by curing the mixture in a flat-bottomed polystyrene Petri dish. The surfaces of the sheets

that were exposed to air during curing were used for the adhesion measurements.

The PDMS ( $\text{HSi}(\text{CH}_3)_2(\text{OSi}(\text{CH}_3)_2)_n(\text{CH}_2)_3\text{CH}_3$ ) chains were grafted to small strips of silicon wafers according to the following method. Small strips of silicon wafers were cleaned in hot piranha solution ( $\text{H}_2\text{SO}_4/\text{H}_2\text{O}_2 = 7:3, \text{v/v}$ ), rinsed in distilled and deionized (DDI) water, and then dried by blowing nitrogen over them. After they were cleaned further in an oxygen plasma for 45 s, they were reacted with  $\text{CH}_2=\text{CH}(\text{CH}_2)_9\text{SiCl}_3$  to form the olefin-terminated self-assembled monolayers using the procedure of vapor-phase adsorption.<sup>9</sup> These silanized silicon strips were then reacted with hydridofunctional PDMS in the presence of a Pt catalyst. A mixture of 0.5 g of polymer and 0.05 g of platinum catalyst was deposited onto the monolayer-coated silicon wafer surface as thin films. After 10 days of grafting, the sample was washed with chloroform in a soxhlet extractor for several hours. For the high-molecular-weight polymer (25 840), heating at 75 °C for overnight was required to ensure good grafting of the polymer. The ellipsometric thicknesses of the grafted PDMS layers are shown in Figure 2.

**Methods to Study Rolling Contact.** Rolling experiments were performed under a microscope with reflection optics (Figure 4). Small sections ( $\approx 2$  mm) were cut out of a long (60 mm) hemicylinder using a razor blade. The cylinders were oxidized in a Harrick plasma cleaner for 45 s at low pressure (0.2 torr) at the low power setting. After these cylinders were equilibrated with the internal humidity of the measuring box, they were brought into contact with the test substrate (Si-PDMS) for a certain amount of time before rolling. The test substrate (Si-PDMS) rested on an analytical balance (Mettler), so that any change of load during rolling could be measured. Cylinders were rolled by tilting one edge of the cylinder with a micromanipulator, controlled by an electrical motor. The rolling speed was controlled by changing the motor speed. The entire rolling process was recorded on a videotape, and the subsequent analysis was carried out with a desktop computer. In order to minimize the effects of humidity, the whole instrument was encased inside a Plexiglass box that was constantly purged with dry air. Dry air was produced by passing the compressed laboratory air through a Whatman purge gas generator, which removed most of organic contamination and moisture. This method ensured the humidity inside the box would remain at about 20% during the experiment.

**Acknowledgment.** Our studies of rolling contact mechanics are based on the prior studies of M. Barquins, whom we thank for sending us the reprints and preprints of the relevant papers. We thank Jim Tonge of Dow Corning Corporation for sending us some of the hydridofunctional silanes used in our studies. We learned about some of the important issues related to the cohesive zone from E. J. Kramer and H. R. Brown through discussions and/or through their previous publications. We thank M. J. Owen and A. Ulman, with whom we had discussions about the H-bonding in PDMS. This work was supported by Dow Corning Corporation, Boeing Airplane Co., and the Office of Naval Research.

## Appendix

It is noteworthy that little hysteresis (Figure 16) is observed in the contact angles of water (Figure 17) on the Si-PDMS surfaces, even though the energy of interaction between water and PDMS is not very different from that at the silica/PDMS interface. Although the hysteresis of wetting energy [ $\gamma_w(\cos \theta_r - \cos \theta_a)$ ] appears to increase

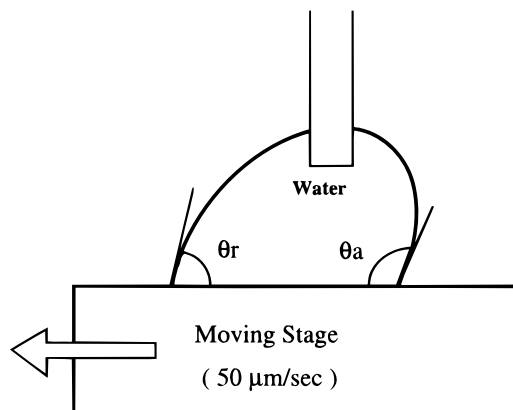


**Figure 16.** Schematic of the method used to measure the advancing and receding contact angles simultaneously. Here, the drop of water is kept stationary and made to roll on the Si-PDMS surface by moving the substrate horizontally at a fixed uniform velocity ( $50 \mu\text{m/s}$ ). The advancing and receding contact angles are measured from the opposite sides of the drop. From the advancing and receding contact angles, the apparent work of adhesion can be calculated as  $W = \gamma_w(1 + \cos \theta)$ , where  $\gamma_w$  is the surface tension of water.

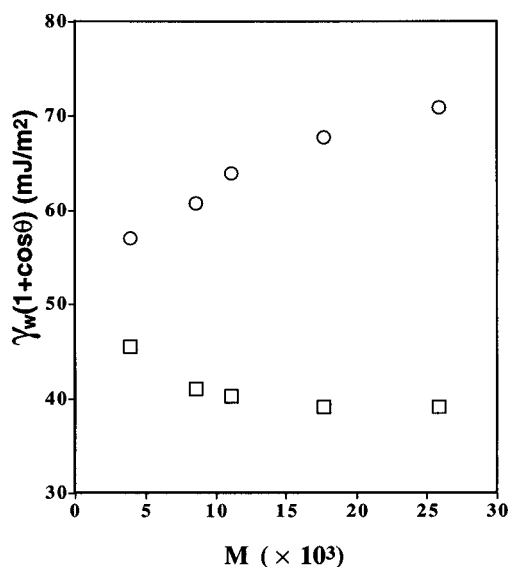


**Figure 17.** Works of adhesion of water on PDMS films of different molecular weights obtained from the advancing ( $\theta_a$ ) and the receding ( $\theta_r$ ) contact angles, respectively.  $\gamma_w$  is the surface tension of water ( $72.8 \text{ mJ/m}^2$ ). (□) and (○) represent advancing and receding contact angles, respectively.

with the molecular weight of the polymer, the values (10–30  $\text{mJ/m}^2$ ) are 1–2 orders of magnitude smaller than those observed (200–2000  $\text{mJ/m}^2$ ) in the rolling contact mechanics experiments. We surmise that the difference of the adhesive hysteresis in the rolling contact mechanics and the contact angle is due to the presence of a significant cohesive zone bridged by polymers in the former case and its absence in the latter.

LA971061M